Received: 30 September 2019 | Revised: 10 December 2019 | Accepted: 10 December 2019

DOI: 10.1111/joa.13150

ORIGINAL PAPER

ANATOMICAL SOCIETY Journal of Anatomy WILEY

Morphological alterations of the reticular thalamic nucleus in Engrailed-2 knockout mice

Andrea Pirone[1] | Cristina Viaggi[2] | Carlo Cantile[1] | Elisabetta Giannessi[1] | Carla Pardini[2] | Francesca Vaglini[2] | Vincenzo Miragliotta[1]

[1]Department of Veterinary Sciences, University of Pisa, Pisa, Italy

[2]Department of Translational Research and of New Surgical and Medical Technologies, University of Pisa, Pisa, Italy

Correspondence
Andrea Pirone, Department of Veterinary Sciences, University of Pisa, Pisa, Italy.
Email: andrea.pirone@unipi.it

Abstract

The reticular thalamic nucleus (Rt) is a sheet of neurons that surrounds the dorsal thalamus laterally, along its dorso-ventral and rostro-caudal axes. It consists of inhibitory neurons releasing gamma-aminobutyric acid (GABA). This nucleus participates in the circuitry between the thalamus and the cerebral cortex, and its impairment is associated with neuro-psychiatric disorders. In this study, we investigated the Rt anatomy of Engrailed-2 knockout mice (*En2*$^{-/-}$), a mouse model of autism spectrum disorder (ASD), using parvalbumin as an immunohistochemical marker. We compared 4- and 6-week-old wild type (WT) and *En2*$^{-/-}$ mice using various morphometric parameters: cell area, shape factor, circularity and cell density. Significant differences were present in 6-week-old male mice with different genetic background (WT vs. *En2*$^{-/-}$): the Rt neurons of *En2*$^{-/-}$ mice showed a bigger cell area, shape factor and circularity when compared with WT. Age (4 weeks vs. 6 weeks) influenced the shape factor of WT females, the circularity and cell density of *En2*$^{-/-}$ males, and the shape factor and circularity of *En2*$^{-/-}$ females. Gender affected cell density in 4-week-old WT mice, shape factor and cellularity of 6-week-old WT mice, and cell area, shape factor and cell density of *En2*$^{-/-}$ at 6 weeks. Intrasubject (left–right) asymmetry of Rt was never observed. These results show for the first time that sex- and age-related changes occur in the Rt GABAergic neurons of the *En2*$^{-/-}$ ASD mouse model.

KEYWORDS

autism spectrum disorder, engrailed, gamma-aminobutyric acid, mouse, parvalbumin, reticular thalamic nucleus

1 | INTRODUCTION

The reticular thalamic nucleus (Rt) is a sheet of neurons that surrounds the dorsal thalamus laterally, along its dorso-ventral and rostro-caudal axes. This nucleus consists of inhibitory neurons releasing gamma-aminobutyric acid (GABA); these neurons mainly contain parvalbumin (PV), even though somatostatin (SOM) immunoreactive cells have been recently described in the rodent Rt (Wells et al. 2016; Clemente-Perez et al. 2017). The Rt plays an important role in the interaction between the thalamus and the cerebral cortex, being depicted as the 'guardian of the gateway' in the thalamocortical circuitry (Crick, 1984). The Rt sends inhibitory projections to and receives excitatory afferents from the thalamocortical circuit, thereby modulating the thalamocortical oscillations on which are grounded relevant functions such as sensorimotor processing, attention, sleep and consciousness (Crick, 1984; Steriade, 2005; Calabrò et al. 2015). Impairment of this circuitry results in neurological and psychiatric disorders (Paz et al. 2010; Ferrarelli & Tononi, 2011).

The Engrailed-2 (*En2*) gene is a homeobox transcription factor that regulates the expression of genes during embryonic and postnatal central nervous system (CNS) development and continues to be expressed in a subset of differentiated neurons in the adult. In

the developing mouse brain, *En2* is mainly expressed in the neural tube where it acts as a patterning gene to determine antero-posterior cell fate identity (Joyner, 1996), regulating cerebellar patterning and connectivity (Joyner et al. 1991; Sillitoe et al. 2010). *En2* gene is essential for the correct development of monoaminergic neurotransmitter pathways. In particular, this gene contributes to mature dopaminergic (DA) neuron survival in normal and Parkinson's disease mouse models (Simon et al. 2005; Sgado et al. 2006; Alavian et al. 2009; Benayed et al. 2009; Alvarez-Fischer et al. 2011; Fox & Deneris, 2012; Viaggi et al. 2015). Mice lacking the *En2* gene present various neuropathological changes including cerebellar hypoplasia, reduced Purkinje cell numbers, disruption of cerebellar patterning and foliation, reduced hippocampal weight, increased dentate gyrus cell turnover, and anterior shift in the position of the amygdala. These neuroanatomical changes are substrates for psychiatric disorders such as autism spectrum disorders (ASD) and schizophrenia. Similarly, $En2^{-/-}$ mice show behavioral abnormalities in social interaction, depression-related tasks, contextual-fear conditioning, spatial memory, seizure threshold and sensory-motor gating (Millen et al. 1994; Cheh et al. 2006; Kuemerle et al. 2007; Tripathi et al. 2009). Since human genetic studies have demonstrated that *En2* is associated with ASD, $En2^{-/-}$ mice are considered a useful neurobiological model of ASD (Gharani et al. 2004; Benayed et al. 2009). Many of the abnormal behaviors shown by $En2^{-/-}$ mice depend on changes in GABAergic neurotransmission; indeed, loss of GABAergic inhibitory neurons has been described in the hippocampus and in different cortical areas of $En2^{-/-}$ mice (Gogolla et al. 2009; Tripathi et al. 2009; Provenzano et al. 2012; Sgadò et al. 2013; Allegra et al. 2014).

In this study, given the role of Rt in the thalamocortical circuitry, we examined whether Rt of 4- and 6-week-old mice (Wild type and $En2^{-/-}$) displayed genetic, sex-related or age-related changes of GABAergic neurons, using immunohistochemistry as an interneuron-specific marker.

2 | MATERIALS AND METHODS

2.1 | Mice

The $En2^{-/-}$ mice were generated as previously described by Joyner et al. (1991). The original *En2* mutants (mixed 129Sv × C57BL/6J and outbred genetic background) were crossed at least five times into a C57BL/6J background. Heterozygous mating ($En2^{+/-}$ × $En2^{+/-}$) was used to generate the $En2^{+/+}$ (wild type, WT) and $En2^{-/-}$ (KO-mice) littermates for this study. The $En2^{-/-}$ status in adult mice was confirmed by tail DNA PCR genotyping according to the protocol available on the Jackson Laboratory website (www.jax.org; mouse strain En2tm1Alj). KAPA Mouse genotyping Kit (KAPA biosystems), consisting of KAPA Express Extract and KAPA2G Fast Genotyping Mix was used for the routine extraction and amplification of DNA for mouse genotyping. Experiments were conducted in conformity with the European Directive of 22 September 2010 (2010/63/UE) and in agreement with the Italian DM26/14. Experiments were approved by the Ethic Committee of the University of Pisa. Forty animals were used in this study, including WT and $En2^{-/-}$ male and female mice (weight = 18–30 g), as shown in Table 1.

TABLE 1 Animal groups used in this study.

Group	Age (weeks)	Sex	*WT*	$En2^{-/-}$	Total no. animals/group
1	4	M	5	5	10
2	4	F	5	5	10
3	6	M	5	5	10
4	6	F	5	5	10

Mice were deeply anesthetized by intraperitoneal (i.p.) injection of chloral hydrate (400 mg kg^{-1}) and perfused through the left ventricle with 200 mL 4% paraformaldehyde in 0.1 M phosphate buffered saline pH 7.4 (PBS). The brain was removed and immersed in 4% paraformaldehyde for 24 h. Transverse brain sections were paraffin embedded and routinely processed for histology.

2.2 | Immunohistochemistry

Immunoperoxidase was performed on serial 5-µm paraffin sections using a mouse monoclonal Anti-PV (1 : 2000, Sigma, P3088, Clone PARV-19). Epitope retrieval was carried out at 120 °C in a pressure cooker for 5 min with a Tris/EDTA buffer, pH 9.0. Sections were pretreated with 1% H_2O_2 in PBS for 10 min to quench endogenous peroxidase activity, then rinsed with 0.05% Triton-X (TX)-100 in PBS (3 × 10 min), and blocked for 1 h with 5% normal horse serum (PK-7200, Vector Labs) in PBS. The sections were then incubated overnight at 4 °C in a solution of anti-PV with 2% normal horse serum and 0.05% TX-100 in PBS. Sections were then rinsed in PBS (3 × 10 min), incubated with biotinylated anti-mouse IgG (5 µg/mL, BA-2001, Vector Labs), and then with ABC reagent (Vectastain Kit, PK-7200, Vector Labs). Sections were again rinsed in PBS (3 × 10 min). Finally, the staining was developed by incubating the sections in diaminobenzidine (sk-4105, Vector Labs) solution. The specificity of immunohistochemical staining was tested using negative control sections, in which the primary antibody, the anti-mouse IgG or the ABC complex was replaced with PBS or non-immune serum. Under these conditions, absence of non-specific staining was confirmed. The specificity of the antibodies has already been tested in previous studies: PV (http://antibodyregistry.org/AB_477329).

2.3 | Image acquisition and processing

Morphometry was performed on three transverse brain sections per animal. To obtain a representative rostro-caudal morphological depiction of Rt, sections corresponding to Bregma −0.8 ± 0.3, −1.4 ± 0.3 and −2 ± 0.3, respectively (Paxinos and Franklin, 2001), were selected. Left and right Rt nuclei were manually drawn at 4× magnification to obtain their area; all immunoreactive cell bodies

TABLE 2 Morphological domains and morphometric indicators, along with their description

Morphological domain	Morphometric indicator	Description
Size	Area	Area of the cell body expressed in μm^2
Shape	Shape factor Circularity	$4\pi \times$ Area/(convex hull perimeter)^2 $4\pi \times$ Area/Perimeter^2

were counted at 10× magnification, and cell density was calculated and expressed as cell number per mm^2. Immunoreactive cells showing a visible nucleus at 40× magnification were segmented by semi-automatic processing, and their area, perimeter, circularity and shape factor collected (Supporting Information Figure S1). While the shape factor was given by the software as $4\pi \times$ Area/(convex hull perimeter)^2, the circularity was manually calculated as $4\pi \times$ Area/Perimeter^2 (Table 2). All measurements and image documentation were performed using the Nikon Ni-e Microscope equipped with the NIS-ELEMENTS BR Software (Nikon Instruments SPA).

2.4 | Statistics

Statistical analysis was performed for all the obtained values to determine intra-subject differences (left–right asymmetry), intra-group

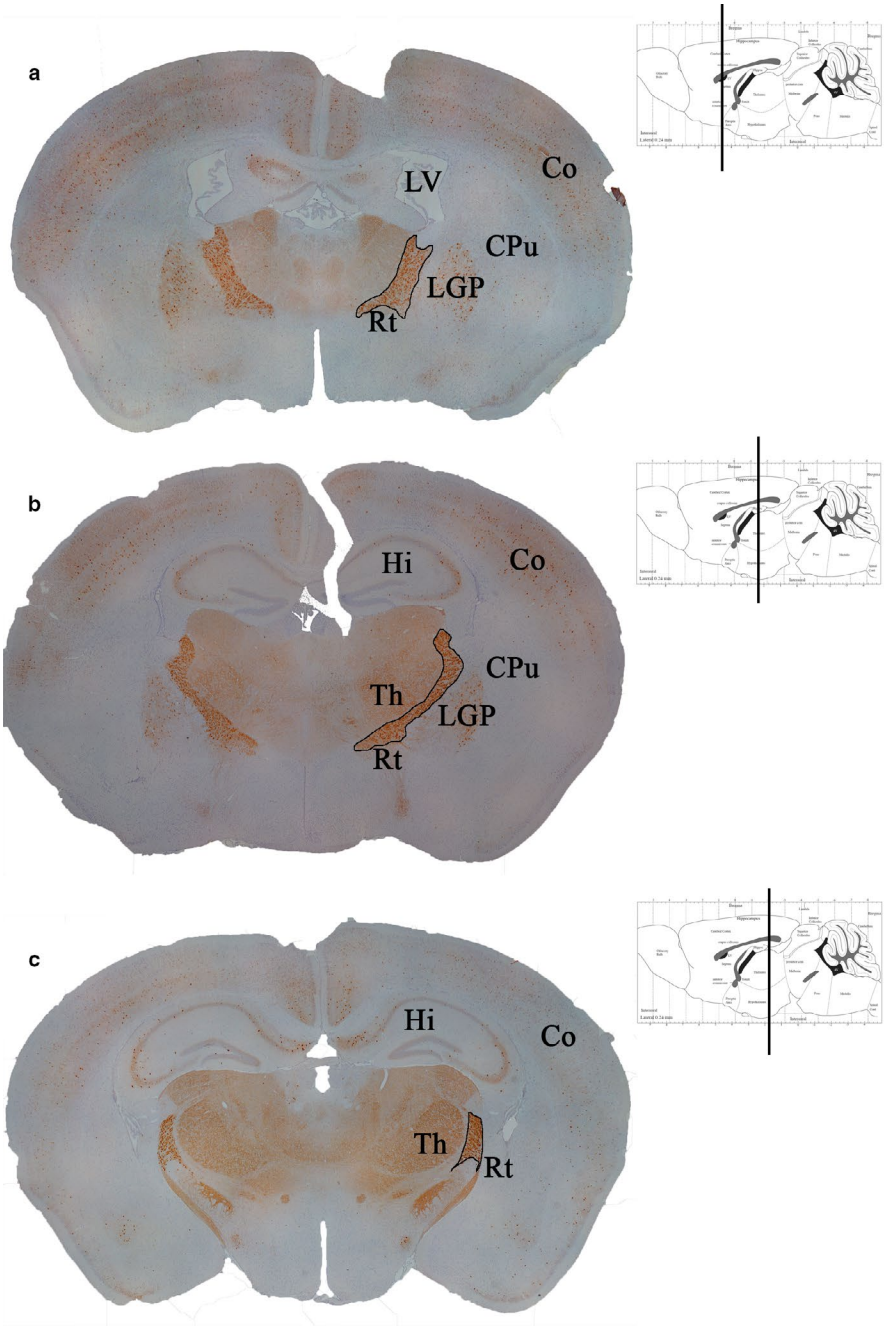

FIGURE 1 Representative images of the three bregma levels used for morphometric analyses of PV immunolabeled Rt: (a) 0.8 ± 0.3, (b) −1.4 ± 0.3, (c) −2 ± 0.3. Drawings on the right indicate the Bregma level according to the mouse brain atlas by Paxinos & Franklin (2001). Rt is encircled by a black line in histological sections. Co, cortex; CPu, caudate-putamen; Hi, hippocampus; LGP, lateral globus pallidus; LV, lateral ventricle; Rt, reticular thalamic nucleus; Th, thalamus.

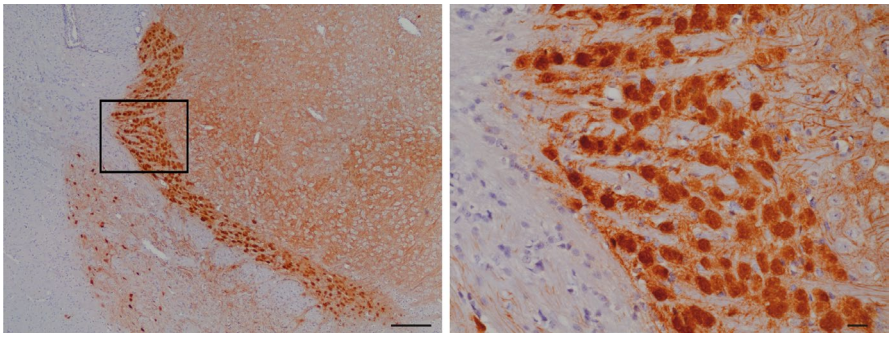

FIGURE 2 Representative section (bregma-1.4 ± 0.3) showing PV immunoreactivity in the Rt. Immunolabeling is mainly localized in the neuronal somata.

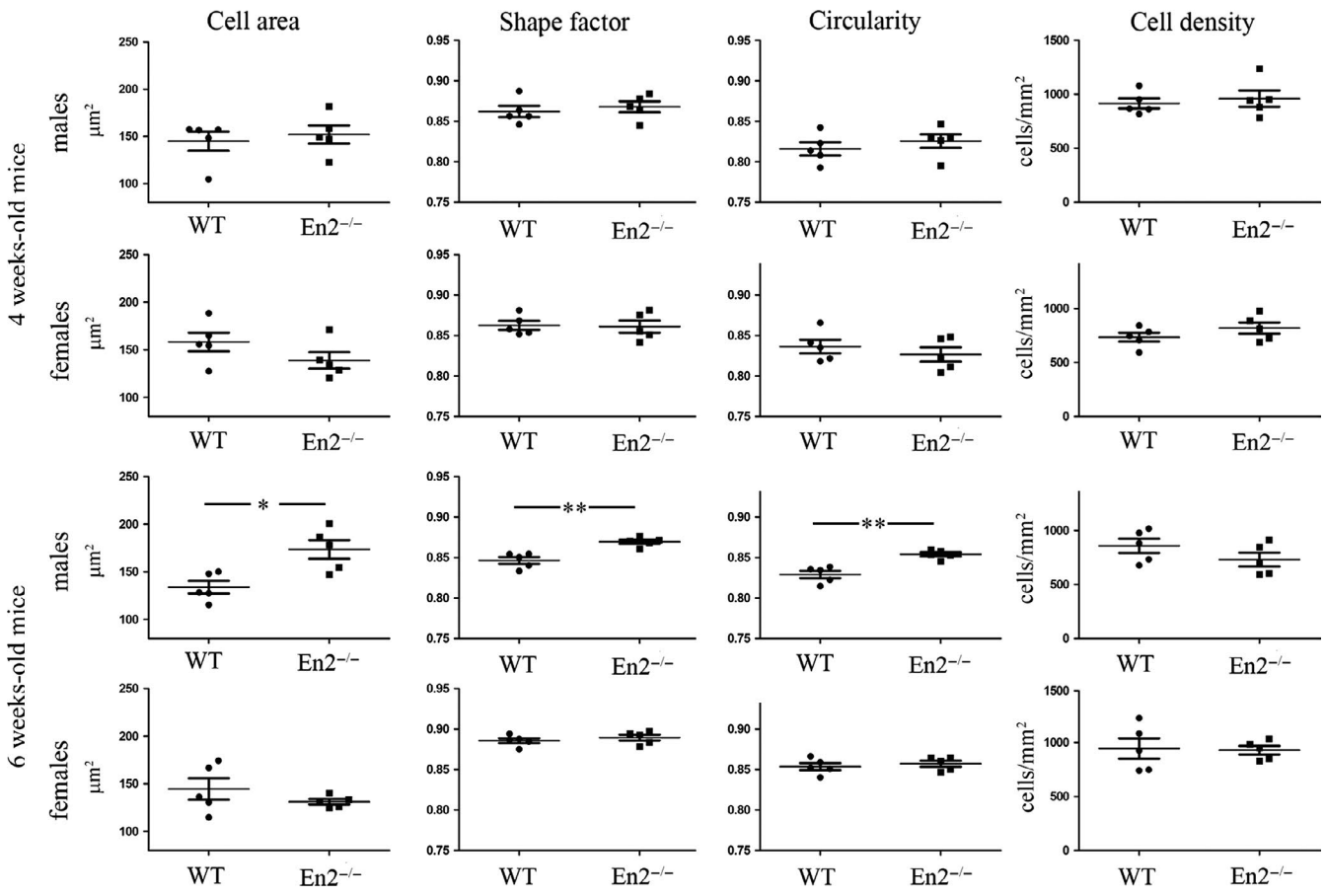

FIGURE 3 Histograms showing differences between wild type (WT) and *En2*$^{-/-}$ mice, of males and females at 4 weeks and 6 weeks of age, on cell area, shape factor, circularity and cell density. Asterisks indicate statistical significance: *P < 0.05; **P < 0.01.

differences (males vs. females) and inter-group differences (WT vs. *En2*$^{-/-}$ and 4-week vs. 6-week-old animals). For intra-subject statistical analysis, a paired *t*-test was used; for all the other comparisons, an unpaired *t*-test was used. Significance was set at $P < 0.05$. Statistical analysis was performed using GraphPad (GraphPad Prism v5.00 for Windows, GraphPad Software).

3 | RESULTS

Immunohistochemical analysis revealed the presence of PV immunoreactive (ir) neurons along the anterior-posterior and dorso-ventral axes of the Rt in both WT and *En2*$^{-/-}$ mice males and females at 4 and 6 weeks of age (Figure 1). Immunostaining was mainly observed in the neuronal soma; PV-positive fibers were rarely seen (Figure 2). Intra-subject (left–right) asymmetry of Rt was not observed.

3.1 | Effect of genotype (WT vs. *En2*$^{-/-}$)

In 4-week-old animals, no differences were observed between WT and *En2*$^{-/-}$ of either sex. The 6-week-old *En2*$^{-/-}$ males showed increased cell area (P = 0.0104), as well as shape factor (P = 0.0014) and circularity (P = 0.0014) when compared with WT animals. The increased size of neurons in *En2*$^{-/-}$ mice corresponded to a decreased cell density in 6-week-old males, although it was not statistically

significant. These changes were not observed in females at the same age. Results are summarized in Figure 3.

3.2 | Effect of age (4 weeks vs. 6 weeks)

Wild-type males did not show age-related changes regarding cell area, shape factor or circularity, whereas WT 6-week-old females displayed a higher shape factor compared with younger mice (P = 0.0064). $En2^{-/-}$ 6-week-old males showed a higher circularity compared with 4-week-old ones (P = 0.112), whereas 6-week-old females displayed both higher shape factor and circularity compared with younger mice (P = 0.093 and 0.0131, respectively). Cell density in WT males did not change significantly with age, whereas it decreased in $En2^{-/-}$ (P = 0.496). The same result was not observed in females, which, however, showed a nearly significant increase in WT (P = 0.768). Results are summarized in Figure 4.

3.3 | Effect of gender (male vs. female)

Four-week-old WT male mice showed a significantly higher cell density compared with females (P = 0.199) which was not maintained at 6 weeks. Conversely, $En2^{-/-}$ animals did not show a gender difference at 4 weeks of age that was instead detectable 2 weeks later, where 6-week-old $En2^{-/-}$ males had a significant lower cell density compared with females (P = 0.294). Whereas at 4 weeks of age the higher cell density observed in WT males was not accompanied by a difference in cell area, the lower cell density of 6-week-old $En2^{-/-}$ males was accompanied by a statistically higher cell area (P = 0.034). Neither WT nor $En2^{-/-}$ mice displayed significant differences in shape factor or circularity at 4 weeks of age. Both shape factor and circularity were lower in males in both WT and $En2^{-/-}$ mice at 6 weeks of age; however, circularity was not statistically different in $En2^{-/-}$ mice. Results are summarized in Figure 5.

4 | DISCUSSION

In this study we showed that the genotype affected only 6-week-old males; in particular the Rt neurons of WT mice showed a smaller cell area, shape factor and circularity. Age influenced the shape factor of WT females, the circularity and cell density of $En2^{-/-}$ males, and the shape factor and circularity of $En2^{-/-}$ females. In addition, gender affected the cell density in 4-week-old WT mice, shape factor and cellularity of 6-week-old WT mice, and the cell area, shape factor and cell density of $En2^{-/-}$ at 6 weeks.

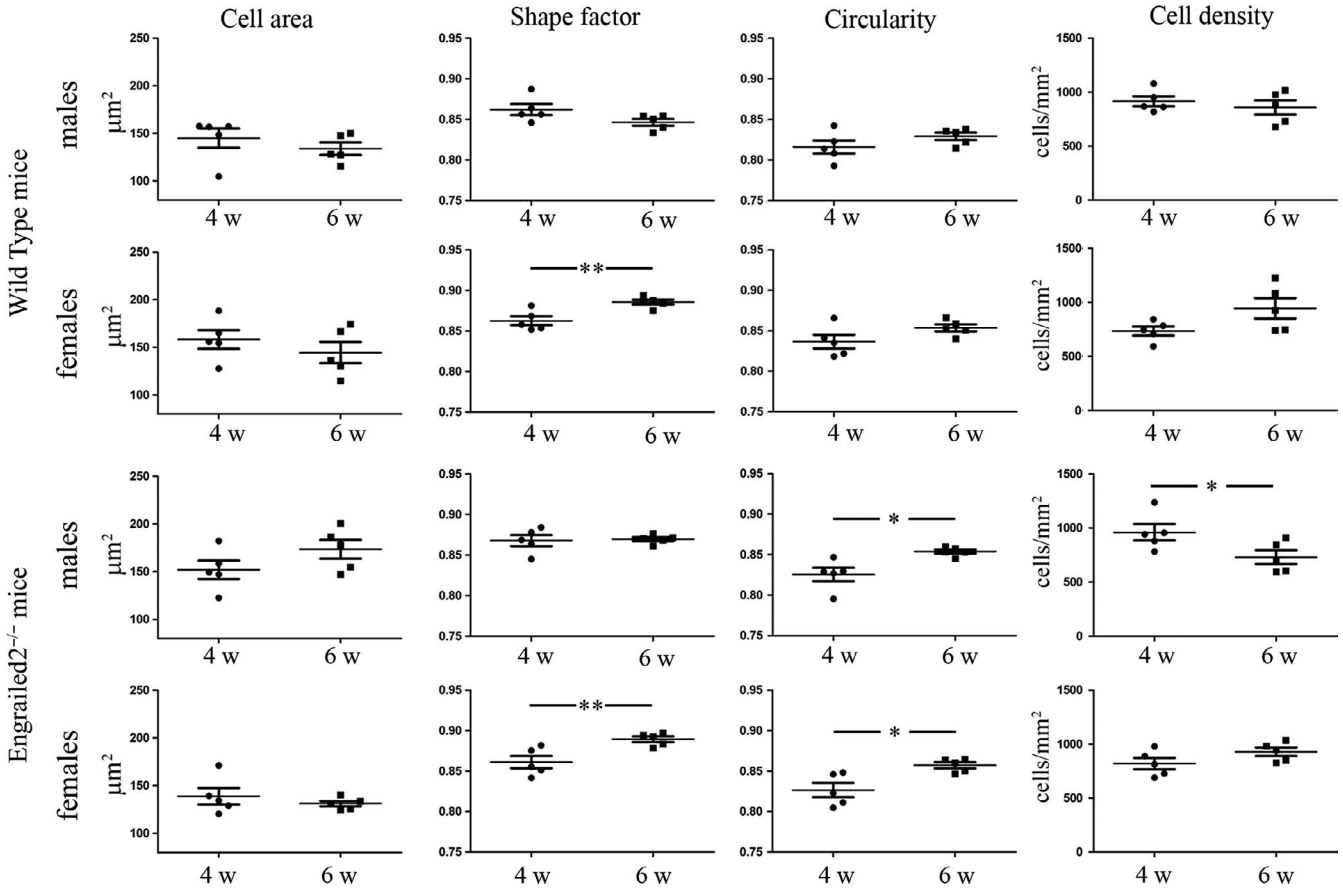

FIGURE 4 Histograms showing differences between 4-week-old and 6-week-old mice, of males and females wild type (WT) and $En2^{-/-}$ genotype, on cell area, shape factor, circularity and cell density. Asterisks indicate statistical significance: *P < 0.05; **P < 0.01.

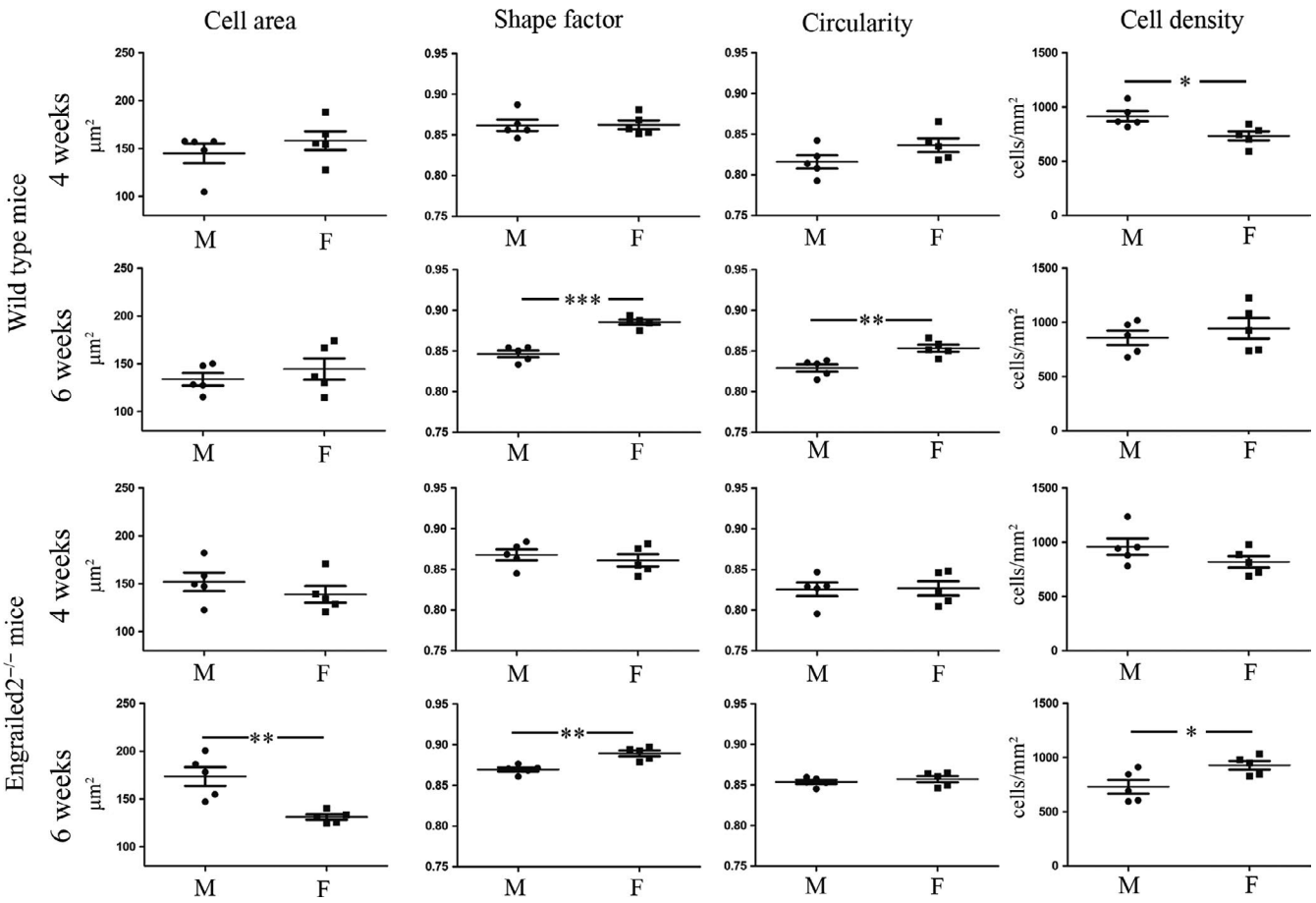

FIGURE 5 Histograms showing differences between male and female mice, of wild type (WT) and *En2*$^{-/-}$ genotype, at 4 weeks and 6 weeks of age, on cell area, shape factor, circularity and cell density. Asterisks indicate statistical significance: **P* < 0.05; ***P* < 0.01; ****P* < 0.001.

4.1 | Genotype (WT vs. En2$^{-/-}$)

In our study, the expression of *En2* was not investigated, thus the morphological alterations observed in Rt could be related to its variations in this anatomical region or induced by *En2* function in adjacent/distant areas (i.e. thalamus and cortical areas) where the *En2* gene is expressed (Brielmaier et al. 2012). In the *En2*$^{-/-}$ mice model, *En2* deletion is known to result in decreased monoamine innervation of target forebrain structures, affecting forebrain growth, postnatal neurogenesis and related behavior (Genestine et al. 2015).

In 6-week-old *En2*$^{-/-}$ males, we detected a higher cell area and a rounder shape of neuronal somata compared with WT. Similarly, PV-labeled Rt neurons became more circular in a rat model of focal infarction of the somatosensory cortex (Paz et al. 2010). Conversely, *En2* expression was shown to induce a reduced size of Purkinje cells soma, in a transgenic mouse model in which *En2* is maintained after birth (Jankowski et al. 2004). Although not directly comparable, in human subjects diagnosed with autism a significant size reduction was found in Purkinje cells, and in frontal and temporal cortex neurons (Casanova et al. 2006; Wegiel et al. 2014a), whereas no changes were described in the amygdala (Wegiel et al. 2014b).

Although we did not find significant differences regarding cell density, reduced PV immunolabeling was detected in adult *En2*$^{-/-}$ mice hippocampus and cerebral cortex (Tripathi et al. 2009; Sgadò et al. 2013). Conversely, an increased number of PV-immunolabeled neurons were reported previously in the visual cortex of the same mice at postnatal day 30 (Allegra et al. 2014). The different brain structures, ages and counting procedures used in other studies might account for these discrepancies.

4.2 | Effect of age (4 week vs. 6 weeks)

En2 is mainly expressed in the developing mouse starting at the neural plate stage and continuing throughout embryonic and postnatal development (Davis & Joyner, 1988; Joyner, 1996; Wilson et al. 2011). However, *En2* mRNA expression was also seen in the adult hippocampus and cerebral cortex (Tripathi et al. 2009; Sgadò et al. 2013), indicating that it may also have a function in these brain areas through the adult age. Our results could support these findings, showing Rt changes in 6-week-old *En2*$^{-/-}$ that were not present at 4 weeks (compared with WT animals). In particular, shape factor was significantly higher at 6 weeks in both WT

and *En2*$^{-/-}$ females, whereas circularity was higher in both genders only in *En2*$^{-/-}$ mice.

The decrease in cell density observed in our study between 4 and 6 weeks of age in *En2*$^{-/-}$ males was also evident in the visual cortex from postnatal day 30 to days 90–120 in a previously reported study on both genotypes (Allegra et al. 2014). However, these data were only barely significant ($P = 0.496$) and the possibility of a type 2 error should not be underestimated.

Although in the present study we did not reveal any age-dependent alteration of cell area, a greater neuronal volume was found in different brain regions of autistic subjects from 11 to 23 and from 36 to 60 years old when compared with younger autistic subjects (Wegiel et al. 2014b).

4.3 | Effect of gender

In the study, we detected gender-related alterations in both WT and *En2*$^{-/-}$ mice. In particular, Rt of 6-week-old WT females showed rounder neuronal somata than those of males of the same age. Moreover, WT females at 4 weeks displayed lower cell density when compared with males. Sex differences have been described in brain structures of non-pathological rodents; for this reason one of the most studied nuclei is named the sexually dimorphic nucleus of the preoptic area, which is smaller and contains fewer neurons than in females (Gorski et al. 1980). Conversely, neurons are more numerous in females than males in the antero-ventral peri-ventricular nucleus, similar to our findings in the Rt nucleus (Simerly et al. 1985).

In *En2*$^{-/-}$ mice, gender-related alterations were present at 6 weeks, but not at 4 weeks. Males were indeed characterized by a higher neuronal cell area and a lower cell density. These gender-related morphological differences have never been reported in studies performed in this mice strain; nor, likewise, have any gender-related differences of behavioral traits and gene expression profiles (Brielmaier et al. 2012; Sgadò et al. 2013; Chelini et al. 2018). However, evidence of gender differences in the brain structure was found in young children with ASD (Retico et al. 2016).

In summary, the present study showed for the first time that changes occur in the Rt GABAergic neurons of *En2*$^{-/-}$ mice of both sexes at 4 and 6 weeks of age. This may lead to abnormal functioning of the Rt, which seems to have a critical role in the regulation of attention in models of autism and neurodevelopmental disorders (Ahrens et al. 2015; Wells et al. 2016; Krol et al. 2018). Some of the obtained results showed only subtle and not statistically significant differences, and others were only slightly statistically different: more studies with a bigger sample size might be helpful to confirm and corroborate the data presented here.

ACKNOWLEDGEMENTS

We are indebted to Sara Degl'Innocenti and Rute Noiva for English revision of the manuscript.

CONFLICT OF INTEREST

This research was conducted in the absence of any commercial or financial relationships that could be construed as potential conflicts of interest.

AUTHOR CONTRIBUTIONS

A.P., V.M., F.V., E.G. conceived the study; A.P., E.G., C.C., C.V., C.P. performed the laboratory experiments; A.P., V.M., F.V., C.V., E.G., C.P. analyzed the data; A.P., V.M. drafted the manuscript; A.P., V.M., F.V., C.C., E.G. revised it critically for important intellectual content. All the authors read and approved the final manuscript.

DATA AVAILABILITY STATEMENT

The data that support the findings of this study are available in the supplementary material of this article.

ORCID

Andrea Pirone https://orcid.org/0000-0001-6363-392X
Vincenzo Miragliotta https://orcid.org/0000-0001-7896-5695

REFERENCES

Ahrens, S., Jaramillo, S., Yu, K., Ghosh, S., Hwang, G.-R., Paik, R., et al. (2015) ErbB4 regulation of a thalamic reticular nucleus circuit for sensory selection. *Nature Neuroscience* 18, 104–111.

Alavian, K.N., Sgadó, P., Alberi, L., Subramaniam, S. and Simon, H.H. (2009) Elevated P75NTR expression causes death of engrailed-deficient midbrain dopaminergic neurons by Erk1/2 suppression. *Neural Development* 4, 1–13.

Allegra, M., Genovesi, S., Maggia, M., Cenni, M.C., Zunino, G., Sgadò, P., et al. (2014) Altered GABAergic markers, increased binocularity and reduced plasticity in the visual cortex of Engrailed-2 knockout mice. *Frontiers in Cellular Neuroscience* 8, 163.

Alvarez-Fischer, D., Fuchs, J., Castagner, F., Stettler, O., Massiani-Beaudoin, O., Moya, K.L., et al. (2011) Engrailed protects mouse midbrain dopaminergic neurons against mitochondrial complex I insults. *Nature Neuroscience*, 14, 1260–1266.

Benayed, R., Choi, J., Matteson, P.G., Gharani, N., Kamdar, S., Brzustowicz, L.M. et al. (2009) Autism-associated haplotype affects the regulation of the homeobox gene, ENGRAILED 2. *Biological Psychiatry* 66, 911–917.

Brielmaier, J., Matteson, P.G., Silverman, J.L., Senerth, J.M., Kelly, S., Genestine, M., et al. (2012) Autism-relevant social abnormalities and cognitive deficits in engrailed-2 knockout mice. *PLoS ONE* 7, 40–42.

Calabrò, R.S., Cacciola, A., Bramanti, P. and Milardi, D. (2015) Neural correlates of consciousness: what we know and what we have to learn! *Neurological Sciences* 36, 505–513.

Casanova, M.F., van Kooten, I.A.J., Switala, A.E., van Engeland, H., Heinsen, H., Steinbusch, H.W.M., et al. (2006) Minicolumnar abnormalities in autism. *Acta Neuropathologica* 112, 287–303.

Cheh, M.A., Millonig, J.H., Roselli, L.M., Ming, X., Jacobsen, E., Kamdar, S., et al. (2006) En2 knockout mice display neurobehavioral and neurochemical alterations relevant to autism spectrum disorder. *Brain Research* 1116, 166–176.

Chelini, G., Zerbi, V., Cimino, L., Grigoli, A., Markicevic, M., Libera, F. et al. (2018) Aberrant somatosensory processing and connectivity in mice lacking Engrailed-2. *Journal of Neuroscience* 39(8), 1525–1538.

Clemente-Perez, A., Makinson, S.R., Higashikubo, B., Brovarney, S., Cho, F.S., Urry, A., et al. (2017) **Distinct** thalamic reticular cell types differentially modulate normal and pathological cortical rhythms. *Cell Reports* 19, 2130–2142.

Crick, F. (1984) Function of the thalamic reticular complex: the searchlight hypothesis. *Proceedings of the National Academy of Sciences of the United States of America* 81, 4586–4590.

Davis, C.A., Joyner, A.L. (1988) Expression patterns of the homeo box-containing genes En-1 and En-2 and the proto-oncogene int-1 diverge during mouse development. *Genes & Development*, 2, 1736–1744.

Ferrarelli, F. and Tononi, G. (2011) The thalamic reticular nucleus and schizophrenia. *Schizophrenia Bulletin*, 37, 306–315.

Fox, S.R. and Deneris, E.S. (2012) Engrailed is required in maturing serotonin neurons to regulate the cytoarchitecture and survival of the dorsal raphe nucleus. *Journal of Neuroscience*, 32, 7832–7842.

Genestine, M., Lin, L., Durens, M., Yan Y., Jiang Y., Prem S. et al. (2015) Engrailed-2 (En2) deletion produces multiple neurodevelopmental defects in monoamine systems, forebrain structures and neurogenesis and behavior. *Human Molecular Genetics*, 24, 5805–5827.

Gharani, N., Benayed, R., Mancuso, V., Brzustowicz, L.M. and Millonig, J.H. (2004) Association of the homeobox transcription factor, ENGRAILED 2, 3, with autism spectrum disorder. *Molecular Psychiatry*, 9, 474–484.

Gogolla, N., LeBlanc, J.J., Quast, K.B., Südhof, T.C., Fagiolini, M. and Hensch, T.K. (2009) Common circuit defect of excitatory-inhibitory balance in mouse models of autism. *Journal of Neurodevelopmental Disorders*, 1, 172–181.

Gorski, R.A., Harlan, R.E., Jacobson, C.D., Shryne, J.E. and Southam, A.M. (1980) Evidence for the existence of a sexually dimorphic nucleus in the preoptic area of the rat. *The Journal of Comparative Neurology*, 193, 529–539.

Jankowski, J., Holst, M.I., Liebig, C., Oberdick, J. and Baader, S.L. (2004) Engrailed-2 negatively regulates the onset of perinatal Purkinje cell differentiation. *The Journal of Comparative Neurology*, 472, 87–99.

Joyner, A.L. (1996) Engrailed, Wnt and Pax genes regulate midbrain-hindbrain development. *Trends in Genetics*, 12, 15–20.

Joyner, A.L., Herrup, K., Auerbach, B.A., Davis, C. and Rossant, J. (1991) Subtle cerebellar phenotype in mice homozygous for a targeted deletion of the En-2 homeobox. *Science*, 251, 1239–1243.

Krol, A., Wimmer, R.D., Halassa, M.M. and Feng, G. (2018) Thalamic reticular dysfunction as a circuit endophenotype in neurodevelopmental disorders. *Neuron*, 98, 282–295.

Kuemerle, B., Gulden, F., Cherosky, N., Williams, E. and Herrup, K. (2007) The mouse Engrailed genes: a window into autism. *Behavioral Brain Research*, 176, 121–132.

Millen, K.J., Wurst, W., Herrup, K. and Joyner, A.L. (1994) Abnormal embryonic cerebellar development and patterning of postnatal foliation in two mouse Engrailed-2 mutants. *Development*, 120, 695–706.

Paxinos, G. and Franklin, K.B.J. (2001) *The Mouse Brain in Stereotaxic Coordinates*, 2nd edn. San Diego: Academic Press.

Paz, J.T., Christian, C.A., Parada, I., Prince, D.A. and Huguenard, J.R. (2010) Focal cortical infarcts alter intrinsic excitability and synaptic excitation in the reticular thalamic nucleus. *Journal of Neuroscience*, 30, 5465–5479.

Provenzano, G., Zunino, G., Genovesi, S., Sgadó, P. and Bozzi, Y. (2012) Mutant mouse models of autism spectrum disorders. *Disease Markers*, 33, 225–239.

Retico, A., Giuliano, A., Tancredi, R., Cosenza, A., Apicella, F., Narzisi, A. et al. (2016) The effect of gender on the neuroanatomy of children with autism spectrum disorders: a support vector machine case-control study. *Molecular Autism*, 7, 1–20.

Sgado, P., Alberi, L., Gherbassi, D., Galasso, S.I., Ramakers, G.M.J., Alavian, K.N. et al. (2006) Slow progressive degeneration of nigral dopaminergic neurons in postnatal Engrailed mutant mice. *Proceedings of the National Academy of Sciences of the United States of America*, 103, 15242–15247.

Sgadò, P., Genovesi, S., Kalinovsky, A., Zunino, G., Macchi, F., Allegra, M. et al. (2013) Loss of GABAergic neurons in the hippocampus and cerebral cortex of Engrailed-2 null mutant mice: Implications for autism spectrum disorders. *Experimental Neurology*, 247, 496–505.

Sillitoe, R.V., Vogel, M.W. and Joyner, A.L. (2010) Engrailed homeobox genes regulate establishment of the cerebellar afferent circuit map. *Journal of Neuroscience*, 30, 10015–10024.

Simerly, R.B., Swanson, L.W. and Gorski, R.A. (1985) The distribution of monoaminergic cells and fibers in a periventricular preoptic nucleus involved in the control of gonadotropin release: Immunohistochemical evidence for a dopaminergic sexual dimorphism. *Brain Research*, 330, 55–64.

Simon, H.H., Scholz, C. and O'Leary, D.D.M. (2005) Engrailed genes control developmental fate of serotonergic and noradrenergic neurons in mid- and hindbrain in a gene dose-dependent manner. *Molecular and Cellular Neurosciences*, 28, 96–105.

Steriade, M. (2005) Sleep, epilepsy and thalamic reticular inhibitory neurons. *Trends in Neurosciences*, 28, 317–324.

Tripathi, P.P., Sgadò, P., Scali, M., Viaggi, C., Casarosa, S., Simon, H.H. et al. (2009) Increased susceptibility to kainic acid-induced seizures in Engrailed-2 knockout mice. *Neuroscience*, 159, 842–849.

Viaggi, C., Gerace, C., Pardini, C., Corsini, G.U. and Vaglini, F. (2015) Serotonin abnormalities in Engrailed-2 knockout mice: new insight relevant for a model of Autism Spectrum Disorder. *Neurochemistry International*, 87, 34–42.

Wegiel, J., Kuchna, I., Nowicki, K., Nowicki, K., Ma, S.Y., Imaki, H. et al. (2014a) Brain-region-specific alterations of the trajectories of neuronal volume growth throughout the lifespan in autism. *Acta Neuropathologica Communications*, 2, 1–18.

Wegiel, J., Flory, M., Kuchna, I., Nowicki, K., Ma, S.Y., Imaki, H. et al. (2014b) Stereological study of the neuronal number and volume of 38 brain subdivisions of subjects diagnosed with autism reveals significant alterations restricted to the striatum, amygdala and cerebellum. *Acta Neuropathologica Communications*, 2, 141.

Wells, M.F., Wimmer, R.D., Schmitt, L.I., Feng, G. and Halassa, M.M. (2016) Thalamic reticular impairment underlies attention deficit in Ptchd1Y/− mice. *Nature*, 532, 58–63.

Wilson, S.L., Kalinovsky, A., Orvis, G.D. and Joyner, A.L. (2011) Spatially restricted and developmentally dynamic expression of engrailed genes in multiple cerebellar cell types. *Cerebellum*, 10, 356–372.

SUPPORTING INFORMATION

Additional supporting information may be found online in the Supporting Information section.

How to cite this article: Pirone A, Viaggi C, Cantile C, et al. Morphological alterations of the reticular thalamic nucleus in Engrailed-2 knockout mice. *J Anat*. 2020;236:883–890. https://doi.org/10.1111/joa13150